Vol. 76, No. 10

Strength of Envelope Protein Interaction Modulates Cytopathicity of Measles Virus

Richard K. Plemper,[1]* Anthea L. Hammond,[1] Denis Gerlier,[2] Adele K. Fielding,[1] and Roberto Cattaneo[1]

Molecular Medicine Program, Mayo Foundation, Rochester, Minnesota 55905,[1] and Immunite et Infections Virales, CNRS-UCBL UMR5537, IFR Laennec, 69372 Lyon Cedex 08, France[2]

To understand the molecular determinants of measles virus (MV) cytopathicity, we have characterized mutant viruses exhibiting a more-extensive cell-to-cell fusion while maintaining efficient replication to high titers. A virus which is modified by the addition of an 8-amino-acid Flag epitope tag at the cytoplasmic tail of its H (for MV hemagglutinin) envelope glycoprotein replicates efficiently, has an increased cytopathicity, possesses a greater infectivity per particle, and has an altered protein composition compared with that of unmodified MV. The mutant phenotype is not specifically linked to the epitope sequence, since an alternatively added HA (for influenza virus-derived hemagglutinin) epitope tag caused similar effects. We demonstrate that both epitope tags weaken the interaction between the H and fusion (F) glycoproteins in virus-infected cells. This reduction in strength of H/F interaction is independent of the presence of the viral matrix (M) protein. Viruses with this less stable complex are more sensitive to neutralization by a soluble octameric form of the CD46 receptor, consistent with their increased fusogenicity. Similar analyses of glycoproteins derived from MV strains with reduced cytopathicities confirm that the strength of H and F glycoprotein interaction is a modulator of viral fusogenicity.

Enveloped viruses that enter target cells through membrane fusion at neutral pH spread through a cell culture both by producing infectious particles and by lateral cell-to-cell fusion. The latter mechanism occurs through binding of viral envelope glycoproteins present at the infected cell surface to a viral receptor(s) on surrounding uninfected cells, thereby inducing membrane fusion, recruiting many cells into a multinucleated syncytium which ultimately dies (16).

The determinants of viral infectivity and the balance between lateral spread and release are complex and incompletely understood. Syncytium formation may be important for viral pathogenesis in vivo. For measles virus (MV), a clinically relevant member of the *Paramyxoviridae*, syncytia have been reported in cells from infected humans (27), primates (29), and transgenic mice (19) expressing one of the virus receptors, CD46 (7, 21). However, syncytia are not produced in every MV-infected tissue, and some primary MV isolates are poorly or nonfusogenic in many cell lines (35). Repeated passaging of the MV-Edmonston (MV-Edm) original isolate on chicken embryo fibroblasts provided the basis for the generation of the MV-Edm B line and the currently used vaccine strains (8, 22, 28), which are no longer pathogenic in vivo. Further adaptation by laboratory passage on cultured primate cells often results in the selection of more fusogenic variants.

Recombinant MVs lacking matrix (M) or the cytoplasmic tail of the fusion (F) protein, mutations found in MV variants causing the rare and fatal complication, subacute sclerosing panencephalitis (17), spread more extensively by cell-to-cell fusion but achieve a significantly lower titer, particularly of released virus (4, 5). Their extended cell-to-cell fusion is a factor facilitating deeper penetration into the brains of CD46-transgenic mice (4), supporting a role for fusogenicity in subacute sclerosing panencephalitis pathogenesis. Furthermore, mutants of murine leukemia virus (10, 36), simian immunodeficiency virus, and human immunodeficiency virus with altered glycoprotein cytoplasmic tails show decreased infectivity (23), increased infectivity (15, 30) or fusogenicity (20), or both increased fusogenicity and infectivity (37). Together, these studies implicate envelope glycoprotein interaction or incorporation as a determinant of viral infectivity.

We now describe the modification of MV particles by the addition of small epitope tags to the H (for MV hemagglutinin) cytoplasmic tail. These viruses induce more-extensive syncytia than does parental MV while they replicate at least as efficiently, depending on the host cell line. Characterizing the basis for this phenotype allows insights into the molecular interactions governing MV infectivity. We demonstrate that addition of the epitope tags weakens the interaction of H with F and that this provides the basis for the observed phenotype. While this effect of the epitope tags is independent of the M protein, it requires the presence of ribonucleocapsid. The correlation between the strength of interaction and cytopathicity was tested for recombinant particles expressing envelope glycoproteins derived from other MV strains with a lateral spread different from that of MV-Edm. Stability of the H/F complexes was found to be an important modulator of virus-induced cell-to-cell fusion.

MATERIALS AND METHODS

Cell culture, transfection, and production of MV stocks. Vero (African green monkey kidney), MA104 (rhesus monkey kidney), HT1080 (human bone fibrosarcoma), and HeLa (human cervical adenocarcinoma) cells were maintained in Dulbecco's modified Eagle's medium containing 10% fetal bovine serum, penicillin, and streptomycin at 37°C and 5% CO_2. Stably transfected 293-3-46 helper

* Corresponding author. Present address: Department of Microbiology & Immunology, Emory University, 3001 Rollins Research Center, 1510 Clifton Rd., Atlanta, GA 30322. Phone: (404) 727-3228. Fax: (404) 727-8250. E-mail: rplempe@emory.edu.

cells (26) were grown in the presence of 1.2-μg/ml Geneticin. For transient transfection, Lipofectamine (Gibco) was used, and cells were analyzed 20 to 24 h posttransfection.

To prepare virus stocks, Vero cells were infected at a multiplicity of infection (MOI) of 0.1 PFU/cell with the relevant virus and incubated at 37°C. Cells were scraped in Opti-MEM (Gibco), and particles released by three freeze-thaw cycles. Titers were determined by 50% tissue culture infective dose ($TCID_{50}$) titration of Vero cells according to the Spearmann-Karber method.

Plasmid construction. The parental plasmids for mutagenesis and all experiments were pCG-H and pCG-F, carrying MV-Edm H and F under the control of the cytomegalovirus promoter (3), and pCG-H_{Flag} (24). Site-directed mutagenesis was performed using the Quick Change system (Stratagene) and confirmed by DNA sequencing and Western analysis.

To transfer tagged H_{Flag} into a DNA copy of the MV genome, *Pac*I/*Spe*I fragments of pCG-H_{Flag} containing the H open reading frame were cloned into *Pac*I/*Spe*I-digested p(+)MV-NSe (31), adhering to the reported rule of six (2). An HA (for influenza virus-derived hemagglutinin) epitope (YPYDVPDYAY)-tagged version of MV-H, pCG-H_{HA}, was generated using primer 5-CTTAGGG TGCAAGATCATCGATAATG**TATCCGTACGACGTCCCGG ATTACGCTT**T CACCACAACGAGACCGGATAAATGC (nucleotides coding for altered or added amino acids are shown in boldface for all primer sequences). Full-length p(+)MV-H_{HA} was generated by transfer of the *Pac*I/*Spe*I fragment from pCG-H_{HA} into p(+)MV-NSe. MV strain Moraten (Moraten) was grown from an aliquot of a currently used vaccine strain, Attenuvax (Merck). To generate a cDNA copy of MV-Edm carrying Moraten-derived glycoproteins, variant amino acids of the Moraten glycoproteins (22) were introduced into pCG-H (positions F117L, N484T, and E600V), using primers 5-CAGAGATTCACTGACCTAGT GAAA**TTA**ATCTCTGACAA GATTAAATTCCTTAATCC, 5-GATTCAAGG TTAGTCCCTACCTC**T**TC**ACT**GTCC CAATTAAGGAAGCAGGCGAAG, and 5-GACATATCACTCACTCTGGGGATG**GTG** GGCATGGGAGTCAGCT GCAC; pCG-F (positions V97 M [14], A166T, R266G, and S365Y), using primers 5-GAACCAATTAGAGATGCACTTAATGCA**ATG**ACCCAGA ATATAA GACCGGTTC, 5-CTGGAAACTACTAATCAGGCAATTGAG**ACA**ATCAG ACAAGCAGGGCAGGAG, 5-GATTTACTGGGCATCTTAGAGAGC**GGA** GGAATA AAGGCCCGGATAACTC, and 5-CTCCAAGAATGCCTCCGGG GGT**TAC**ACTAAGT CCTGTGCTCGTACAC. The *Pac*I/*Spe*I fragment from pCG-H_{Mor} and the *Nar*I/*Pac*I fragment from pCG-F_{Mor} were cloned into p(+)MV-NSe. To generate a cDNA copy of p(+)MV-H_{Flag} lacking most of the M coding region, the 10,696-bp *Sac*II/*Pac*I fragment of p(+)MV-H_{Flag} was ligated with the *Sac*II/*Pac*I fragment of p(+)MV-ΔM (4) harboring the M gene deletion.

Recovery of recombinant viruses. Recombinant MVs were generated essentially as described (26). Briefly, the helper cell line 293-3-46 stably expressing MV-N, MV-P, and T7 polymerase was transfected by calcium phosphate precipitation with the ProFection kit (Promega) with a DNA copy of the relevant MV genome and MV polymerase L. Helper cells were overlaid on Vero cells 76 h posttransfection, and the resulting infectious centers were passaged on Vero cells. In all cases, the integrity of recombinant viruses was confirmed by reverse transcription-PCR and DNA sequencing of the modified genes.

Western analysis. Cells (4×10^5) were infected at an MOI of 0.1 PFU/cell, washed 36 h later in phosphate-buffered saline, lysed for 10 min at 4°C in lysis buffer (50 mM Tris [pH 8.0], 62.5 mM EDTA, 0.4% deoxycholate, 1% Igepal [Sigma]) containing protease inhibitors (Complete mixture [Roche]) and 1 mM phenylmethylsulfonylfluoride (PMSF), and centrifuged at $5,000 \times g$ for 10 min at 4°C. The total protein concentration of postnuclear supernatants was determined using the DC Protein Assay kit (Bio-Rad). Unless otherwise stated, 2.5 μg of total protein was mixed with urea buffer (200 mM Tris [pH 6.8], 8 M urea, 5% sodium dodecyl sulfate, 0.1 mM EDTA, 0.03% bromphenol blue, 1.5% dithiothreitol) for 25 min at 50°C. Samples were fractionated on sodium dodecyl sulfate-polyacrylamide gels, blotted to polyvinylidene difluoride membranes (Millipore), and subjected to enhanced chemiluminescence detection (Amersham Pharmacia Biotech) using antibodies specific for the Flag epitope (M2; Sigma), MV-N and -M (both Chemicon), the cytosolic tails of H and F (24), and the ectodomain of F, as indicated.

Virus growth kinetics. Vero cells (4×10^5 per time point) were infected at an MOI of 0.03 PFU/cell. At the indicated time points, supernatants were cleared by centrifugation, cells were scraped in Opti-MEM (Gibco) and subjected to freeze-thaw cycles, and released and cell-associated titers were determined by $TCID_{50}$ titration. Where indicated, 2.5 μg of total lysate protein was subjected to Western analysis to follow synthesis of viral proteins.

Metabolic labeling and purification of viral particles. Vero cells were infected at an MOI of 0.1 PFU/cell and incubated for 30 h and then for 20 h in labeling medium lacking cysteine, methionine, and ammonium sulfate supplemented with

1% fetal bovine serum and 100-μCi/ml [^{35}S]methionine (Amersham Pharmacia Biotech). Labeled particles were purified essentially as described (24). Briefly, supernatants were cleared by centrifugation at $20,000 \times g$ at 4°C for 20 min. Viral particles were concentrated at the interphase of a 20 and 60% sucrose gradient in TNE buffer (10 mM Tris [pH 7.8], 100 mM sodium chloride, 1 mM EDTA) by centrifugation at $100,000 \times g$ at 4°C for 90 min and then diluted with TNE buffer to less than 30% sucrose. Particles were pelleted at $100,000 \times g$ at 4°C for 90 min, resuspended in TNE buffer, and subjected to $TCID_{50}$ titration and, after addition of urea buffer, to Western analysis. Labeling efficiency was determined by analysis of purified particles with a scintillation counter.

Coimmunoprecipitation. Cells were cotransfected with 2.5 μg each of plasmid DNA encoding MV-F and -H or MV-H_{Flag} as indicated or virus infected at an MOI of 0.1 PFU/cell. For some experiments, fusion inhibitory peptide (FIP) was added at a final concentration of 200 μM 12 h postinfection. After being washed with phosphate-buffered saline, cells were scraped in coimmunoprecipitation buffer (10 mM HEPES [pH 7.4], 50 mM sodium pyrophosphate, 50 mM sodium fluoride, 50 mM sodium chloride, 5 mM EDTA, 5 mM EGTA, 100 μM sodium vanadate, 1% Triton X-100) containing protease inhibitors (Complete mixture) and 1 mM PMSF. Lysates were cleared by centrifugation for 25 min at $20,000 \times g$ and 4°C, and 300 μg of total protein was incubated with antibodies directed against MV H (Chemicon) for 90 min at 4°C. As an internal standard, 5 μg of total protein was mixed with urea buffer. Immune complexes were adsorbed to protein G-agarose (GibcoBRL) for 90 min at 4°C, washed in buffer 1 (100 mM Tris [pH 7.6], 500 mM lithium chloride, 0.1% Triton X-100, 1 mM dithiothreitol) and then buffer 2 (20 mM HEPES [pH 7.2], 2 mM EGTA, 10 mM magnesium chloride, 0.1% Triton X-100, 1 mM dithiothreitol), incubated in urea buffer for 25 min at 50°C, and subjected to Western analysis using antibodies specific for MV-F tail or ectodomain as indicated.

Neutralization assays. Viral particles, corresponding to an MOI of 0.1 PFU/cell, were incubated with indicated concentrations of sCD46-C4bpα molecules (6) for 1 h at 37°C in Opti-MEM, absorbed to Vero cells for 90 min at 37°C, and incubated for 48 h after the addition of Dulbecco's modified Eagle's medium and 10% fetal calf serum. For harvesting, cells were scraped in Opti-MEM and subjected to three freeze-thaw cycles. A total of 2.5 μg of total protein was used for Western analysis, and cleared viral lysates were subjected to $TCID_{50}$ titration.

RESULTS

MV-Edm carrying a Flag epitope at the cytoplasmic tail of H induces more-extensive syncytia and replicates efficiently to high titers. When an 8-amino-acid Flag epitope was added to the N terminus of MV-Edm H, a recombinant MV-H_{Flag} virus was rescued which induced syncytium formation earlier and significantly more extensively than did unmodified MV-Edm (Fig. 1A).

In repeated time courses in Vero cells, MV-H_{Flag} consistently replicated to final titers at least as high as those of the parental untagged virus. In several independent experiments, maximum titers of cell-associated and released viral particles were increased on average by 1 logarithmic unit over the parental strain (Fig. 1B). The slope of the growth curves did not differ significantly between the two viruses. This was consistent with a similar transport kinetics of H-H_{Flag} and H-Edm, previously observed when the transiently expressed protein was analyzed (11).

When equal amounts of total protein from cell lysates were analyzed at each time point by Western blotting, H was more abundant in MV-H_{Flag}- than MV-Edm-infected cells (Fig. 1C). Surprisingly, H_{Flag} was detectable 6 h earlier in cells infected with the mutant virus. Considering the very similar growth kinetics of the two viruses, this may reflect differences in cell entry. The presence of the Flag epitope was confirmed by Western analysis with an anti-Flag antibody.

Importantly, when transiently coexpressed with MV-F protein in Vero cells, H-Edm_{Flag} induced a level of syncytium formation similar to that of H-Edm (data not shown).
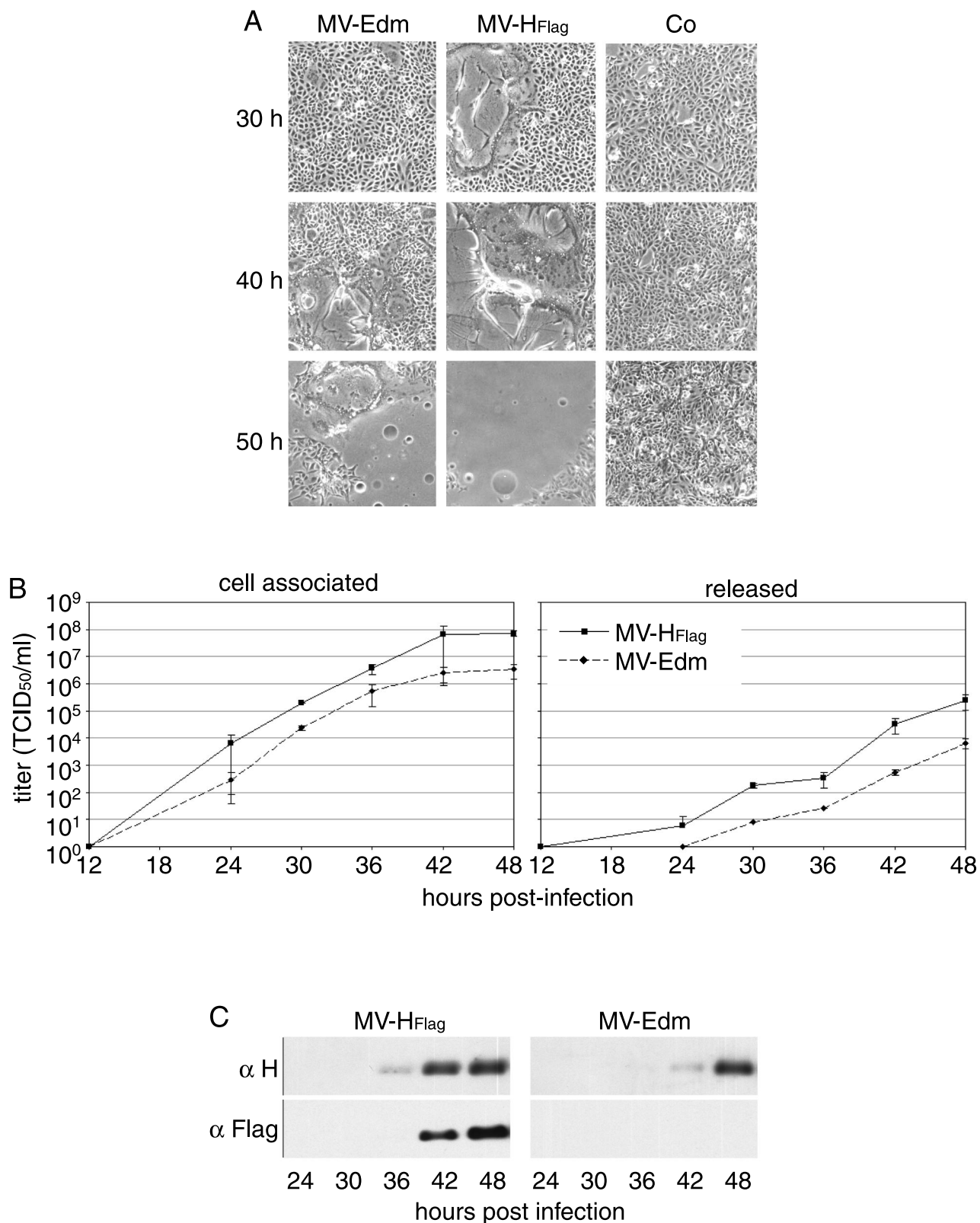
FIG. 1. Addition of the Flag epitope to the cytoplasmic tail of H results in increased fusogenicity. (A) Representative fields of view of Vero cells infected with MV-Edm and MV-H$_{Flag}$ (MOI = 0.03 PFU/cell) or uninfected (Co), at indicated times postinfection. (B) Growth kinetics of MV-Edm and MV-H$_{Flag}$ in Vero cells. Cells were infected at an MOI of 0.03 PFU/cell. At the indicated time points, titers were determined for both cell-associated and released viral particles. (C) Western analysis of total cell lysates derived from the experiment shown in panel B using anti-H and Flag antibodies.
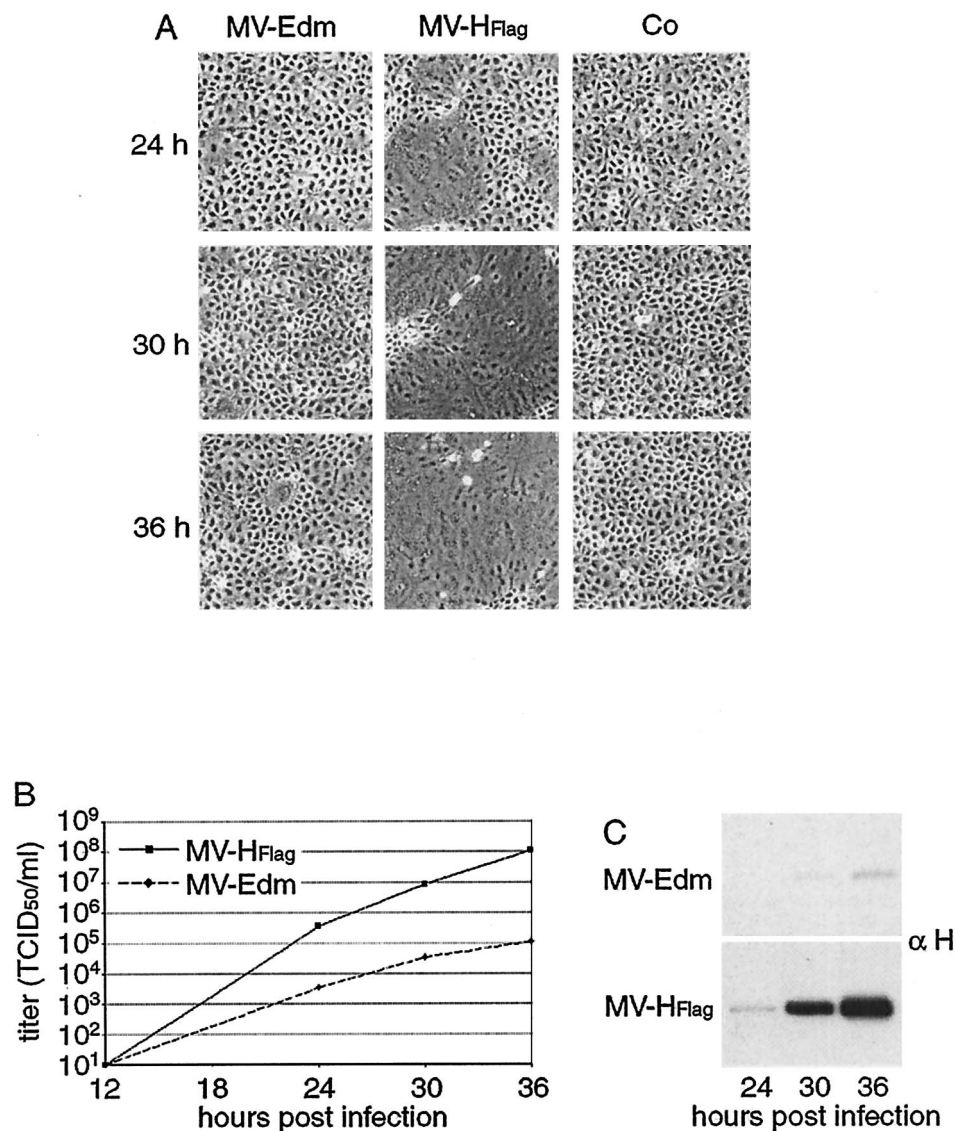
FIG. 2. The phenotype of MV-H$_{Flag}$ is not Vero cell dependent and is most pronounced in MA104 cells. (A) Representative fields of view of MA104 cells infected with MV-Edm and MV-H$_{Flag}$ or uninfected (Co), at indicated hours postinfection. (B) Growth kinetics of MV-Edm and MV-H$_{Flag}$ in MA104 cells. Cells were infected at an MOI of 0.03 PFU/cell. At the indicated time points, titers of cell-associated viral particles were determined. (C) Western analysis of total cell lysates derived from the experiment shown in panel B using anti-H antibodies.

The phenotype of MV-H$_{Flag}$ is neither Vero cell nor Flag epitope dependent. The phenotype of MV-H$_{Flag}$ was studied with other CD46-positive cell types to investigate its general relevance. Syncytium formation in HeLa, HT1080 (data not shown), and MA104 cells was also more efficiently induced by MV-H$_{Flag}$, as shown in Fig. 2A for MA104 cells, which displayed the most pronounced difference. In this cell line, MV-H$_{Flag}$ reached a significant difference in titer compared with MV-Edm and displayed a faster kinetics of virus growth (Fig. 2B). Western blot analysis of infected MA104 cells following the level of MV-H protein at each time point (Fig. 2C) mirrored the growth curves, showing a far greater level of H expression from MV-H$_{Flag}$-infected cells. That this cell line replicated faster than Vero cells may reflect differences in cellular factors which contribute to the productivity of viral infection.

To investigate whether the phenotype of MV-H$_{Flag}$ was specific to the sequence of the Flag epitope or whether the extension of H tail per se was responsible, we replaced the Flag tag with a 10-amino-acid HA epitope. Following rescue of the MV-H$_{HA}$ virus, it too was found to induce more massive syncytium formation than MV-Edm in MA104 cells, as shown in Fig. 3A. Furthermore, it replicated as efficiently as MV-Edm in Vero cells (data not shown) and reached significantly greater endpoint titers in MA104 cells (Fig. 3B). Thus, the phenotype of MV-H$_{Flag}$ is not peculiar to the sequence of the appended tag.

MV-H$_{Flag}$ particles show an altered protein composition, a more efficient release, and a greater infectivity per particle than MV-Edm. To investigate whether the modified H protein affected the efficiency of incorporation of other viral proteins into particles and thus the assembly process, we compared the
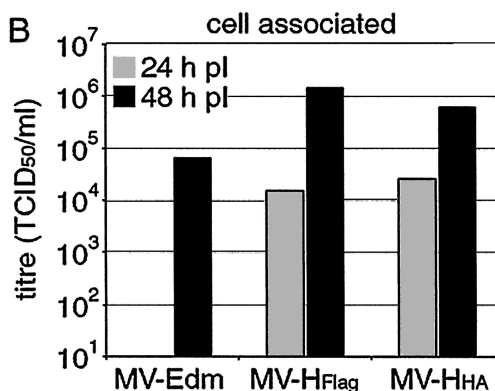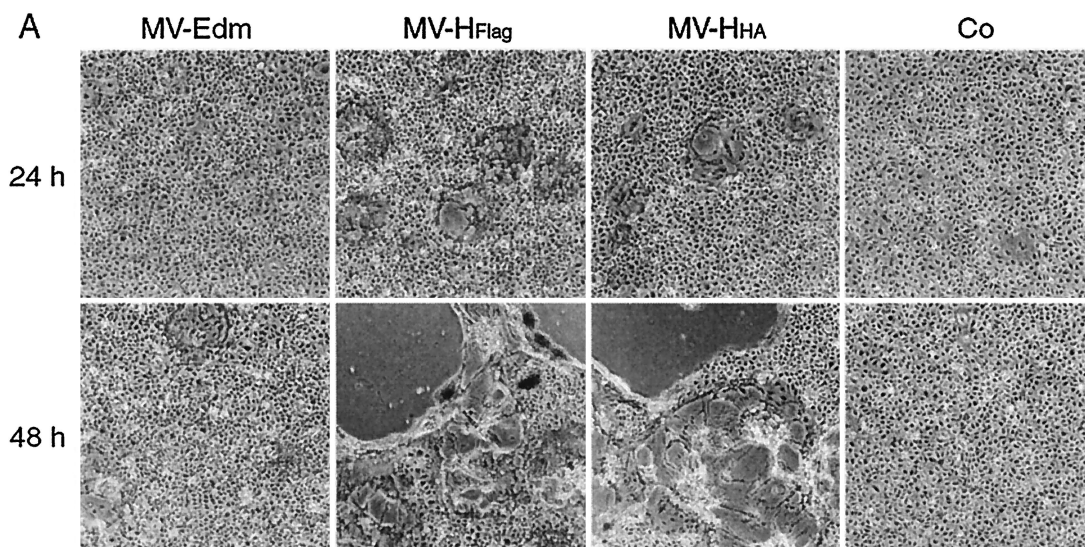
FIG. 3. The mutant phenotype is not sequence restricted. (A) Representative fields of view of MA104 cells infected with MV-Edm, MV-H$_{Flag}$, and MV-H$_{HA}$ or uninfected (Co) at indicated hours postinfection. (B) Endpoint titration of viruses derived from the cells shown in panel A. Titers of cell-associated virus were determined in duplicate.

compositions of MV-H$_{Flag}$ and MV-Edm particles. Released viral particles were purified from the extracellular supernatant of infected cells, subjected to TCID$_{50}$ titration, and analyzed by Western blotting with anti-MV sera recognizing N, H, F, and M proteins (Fig. 4A).

The purified viral particle preparations were normalized for equal quantities of the N protein, based on the assumption that the number of N proteins per genome (which is estimated to have 3,000 proteins per genome in analogy to Sendai virus [32]), might be unaffected by the modification of H. In relation to N, MV-H$_{Flag}$ particles contained drastically elevated levels of M, slightly increased levels of F, and slightly decreased levels of H protein compared to MV-Edm.

Since it is unknown whether normalizing for N equates to similar numbers of particles, we also analyzed infectivity after standardization based on metabolic labeling of total viral proteins by [^{35}S]methionine and purification of released particles. The infectious titer associated with labeled particles was determined by TCID$_{50}$ titration and expressed as the number of PFU per counts per minute (Fig. 4B). Using this assay, the infectivity per particle of purified MV-H$_{Flag}$ was about 1,000-fold greater than that of MV-Edm, roughly mirroring the data obtained when normalizing for N.

Interaction of tagged H-Edm with F-Edm is weaker than that of unmodified H in the context of viral infection. Considering our recent observation that the MV-F and -H proteins intracellularly form stable hetero-oligomers (25), it seemed possible that the epitope tags added to the H terminus interfere with glycoprotein complex formation either directly or indirectly through an interaction with M; either might provide
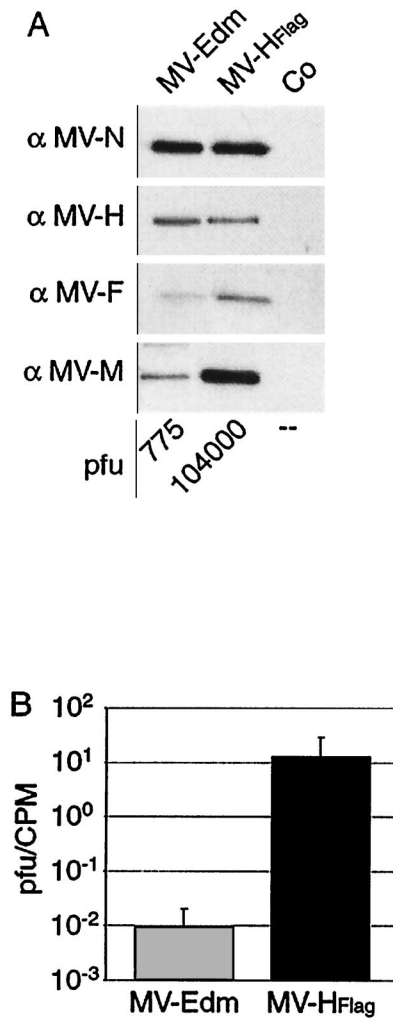
FIG. 4. MV-H$_{Flag}$ has an altered protein composition and a greater infectivity per particle than MV-Edm. (A) Composition of purified MV-Edm and MV-H$_{Flag}$ particles released from Vero cells. Particles were purified by sucrose centrifugation and subjected to Western analysis with sera derived against N, H, F, and M. Total amounts of infectious particles (PFU) associated with each preparation are indicated. Co, control. (B) Infectivity per released particles of purified MV-Edm and MV-H$_{Flag}$, expressed as the number of PFU per counts per minute. Radiolabeled particles were purified and subjected to scintillation counting to determine counts per minute, and TCID$_{50}$ titration was carried out to determine the number of infectious particles per preparation.
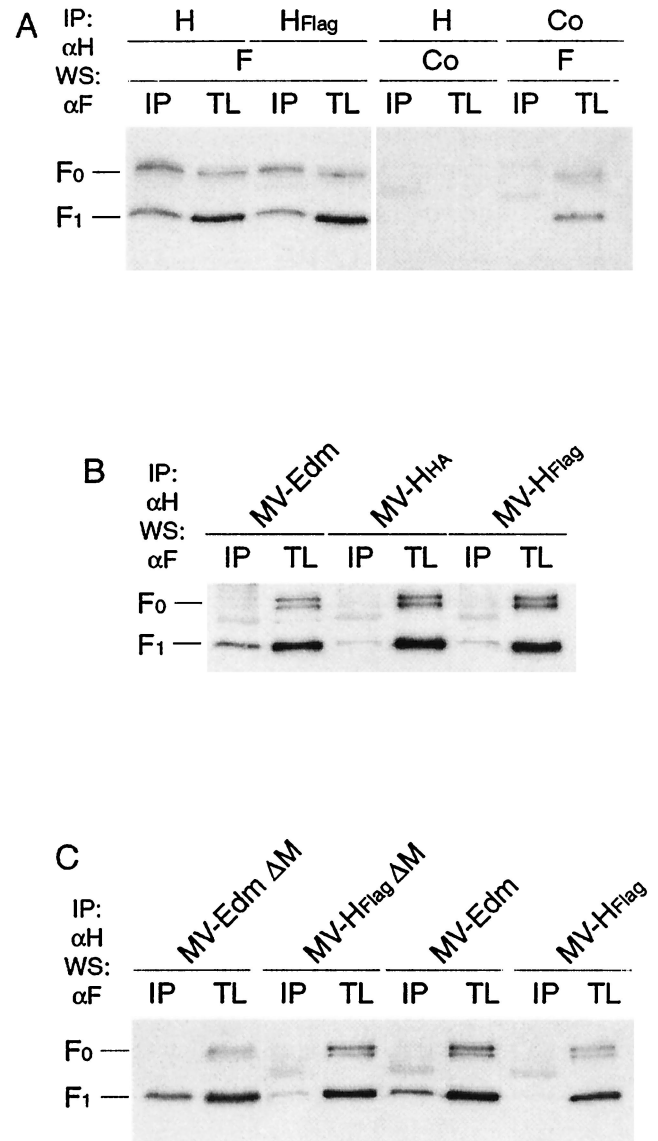

FIG. 5. Interaction of H$_{Flag}$ with F is weaker than that of H with F in the context of viral infection. (A) Coimmunoprecipitation of F with H or H$_{Flag}$ following transient expression in Vero cells. F antigenic material from coimmunoprecipitated (IP) samples and total cell lysate (TL) was detected by Western analysis (WS) using specific antibodies directed against the cytosolic F tail. Control (Co) transfection was with equal amounts of noncoding plasmid DNA. (B) Coimmunoprecipitation of F with H from Vero cells infected with the indicated viruses at an MOI of 1.0 PFU/cell. (C) Analysis of MV recombinants lacking the M protein. Coimmunoprecipitation of F with H as in the results shown in panel B.

the basis for the observed higher fusogenicity. To biochemically test this hypothesis, we carried out coimmunoprecipitation experiments using an antibody directed against the MV-H ectodomains, followed by Western blot analysis of the precipitates using an anti-F antibody. Comparing the amount of F which coimmunoprecipitated with H with that present in the total cell lysate as an internal standard enables calculation of the relative efficiency of the coimmunoprecipitation and thus of the strength of H/F interaction.

In cells transiently expressing F and H-Edm or F and H-Edm$_{Flag}$, no differences could be observed in the strength of interaction between H and F proteins (Fig. 5A), in line with the

indistinguishable biological activity of these two proteins. When this was assessed in the context of an infection, significantly less F could be coimmunoprecipitated with H$_{Flag}$ than with H although more F was present in MV-H$_{Flag}$- than in MV-Edm-infected cells (Fig. 5B). Thus, when the epitope tag results in a phenotypic difference (i.e., in virus-infected cells), a significantly less stable complex of the tagged H with MV-F protein is formed. To confirm that modification of the cyto-

plasmic tail of MV-H caused a destabilization of the complex, we also compared the interaction between H_{HA} and F by coimmunoprecipitation and found it also to be weaker than that between H-Edm and F in cells infected with MV-H_{HA} and MV-Edm, respectively (Fig. 5B). Thus, it is the addition of an epitope tag to the cytosolic tail of H which causes the weakened interaction between H and F.

It was conceivable that the MV-M protein accounts for this difference in glycoprotein complex stability in the context of viral infection compared to transient expression of H and F. M has been shown to physically interact with ribonucleocapsid (13, 34) and the cytosolic tail of F (33). When transiently coexpressed with H and F in previous studies, however, M failed to affect fusion probably due to the absence of ribonucleocapsids (T. Cathomen and R. Cattaneo, unpublished observations). To test a potential contribution of M to glycoprotein complex stability we therefore generated and recovered MV particles expressing the tagged H protein but lacking M. This MV-H_{Flag} ΔM recombinant was confirmed through DNA sequencing and Western analysis (data not shown). Lysates of cells infected with either MV-H_{Flag} ΔM, MV-Edm ΔM (4), MV-H_{Flag}, or MV-Edm were subjected to coimmunoprecipitation of F with H. The difference in coprecipitation efficiency between H or H_{Flag} and F was unchanged regardless of the presence or absence of M (Fig. 5C). Interestingly, in both ΔM recombinant strains the glycoprotein complex stability was slightly increased, rather than decreased, compared to the corresponding parental strains carrying the M gene. Thus, the absence of M does not influence the effect caused by the epitope tags. Presumably, the difference in H_{Flag}/F complex stability in the context of viral infection is due to the presence of ribonucleocapsid rather than the M protein alone.

MV-H_{Flag} shows increased sensitivity to neutralization by soluble CD46. We speculated that the weakened interaction between H_{Flag} and F facilitates a more efficient infection by rendering the H/F glycoprotein complex prone to fusion. Since it is most likely that the MV entry cascade is initiated by receptor binding inducing conformational changes in H and then F, H_{Flag}/F-containing complexes may conceivably be in an altered conformational state facilitating receptor binding. H/F complexes in such a conformation may be highly sensitive to neutralization by soluble receptor molecules. To test this hypothesis, we compared the sensitivity of MV-Edm and MV-H_{Flag} to octameric sCD46-Cpbα molecules, previously shown to neutralize MV-Edm irreversibly and much more efficiently than monomeric sCD46 or antibodies derived against the MV glycoproteins (6).

Consistent with previous data, infection of Vero cells by MV-Edm was inhibited in a dose-dependent fashion by sCD46-Cpbα (Fig. 6A). MV-H_{Flag} was, however, far more sensitive to neutralization by the soluble receptor, as apparent from the inhibition curves. These findings were mirrored by the expression levels of H protein from the infected cells determined 48 h postinfection. After pretreatment of MV-H_{Flag} with increasing concentrations of sCD46-Cpbα, H levels decreased rapidly (Fig. 6B). In contrast, cells infected with pretreated MV-Edm revealed a far more moderate decrease in H expression. Thus, the weakened interaction between H_{Flag} and F results in an increase in sensitivity to neutralization, consistent with this glycoprotein complex resembling an activated conformational state.
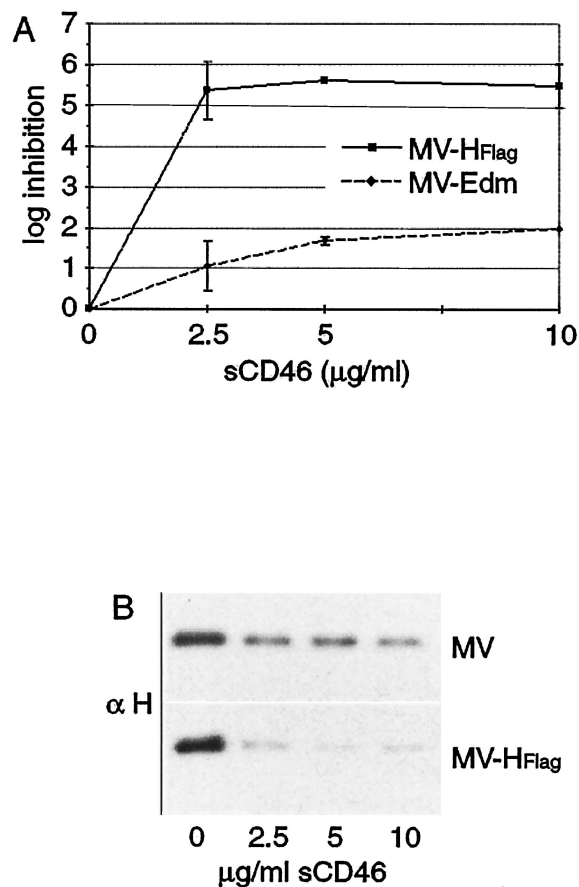

FIG. 6. Inhibition of infection through soluble sCD46-Cpbα molecules. (A) Cells were infected with the indicated viruses at an MOI of 0.1 PFU/cell in the presence of sCD46-Cpbα molecules, and cell-associated particles were harvested 48 h postinfection and subjected to TCID$_{50}$ titration. (B) Western analysis with anti-H antibodies of cell lysates derived from the cells shown in panel A.

MV-Moraten-derived glycoproteins induce less cell-to-cell fusion and interact very efficiently. We investigated whether the observed correlation between MV-H_{Flag}- and MV-H_{HA}-induced cell-to-cell fusion and reduced strength of H-F interaction was limited to the recombinant epitope tagged strains or extended to other MV strains. Therefore, we analyzed glycoproteins derived from a current vaccine strain, MV-Moraten (12). This strain was selected because we found cytopathicity of MV-Moraten to be very different from that of MV-Edm, inducing only small syncytia and causing extensive cell rounding with increasing time of infection. To assess the contribution of the F and H proteins to this phenotype, we constructed and recovered a virus carrying the F and H proteins of MV-Moraten in place of those of MV-Edm, but otherwise genetically identical to MV-Edm, which was designated MV-Edm-H/F-Moraten.

When comparing growth of MV-Edm, MV-Moraten, and MV-Edm-H/F-Moraten in Vero cells (Fig. 7A), MV-Edm induced cell-to-cell fusion which lysed all cells about 48 h postinfection. In contrast, both MV-Moraten and MV-Edm-H/F-Moraten induced cytopathicity, based predominantly on rounding of individual cells rather than cell-to-cell fusion. Ti-
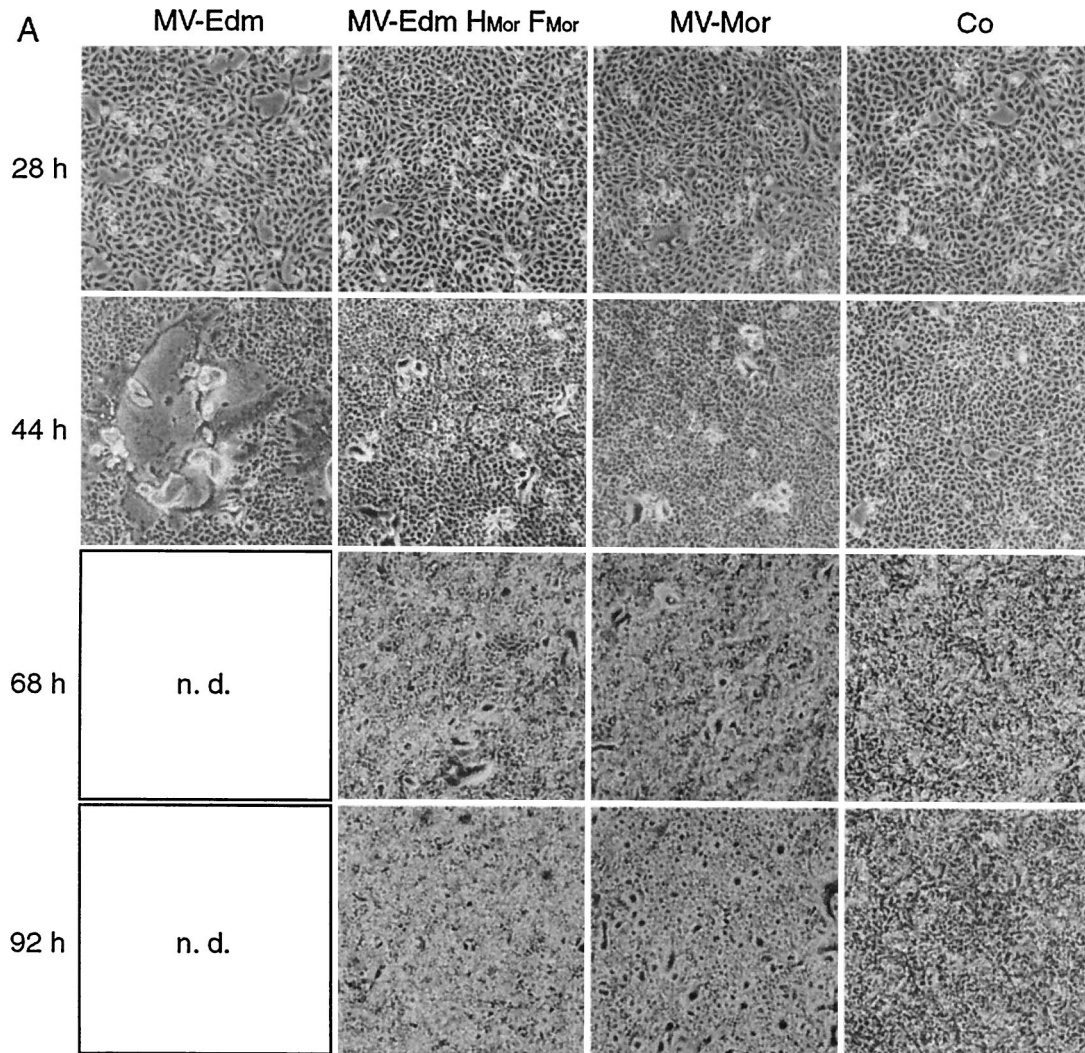
FIG. 7. Strength of MV glycoprotein interaction is a determinant for viral cytopathicity. (A) Representative fields of view of Vero cells infected with MV-Edm, MV-Edm-H/F-Moraten, and MV-Moraten (MOI = 0.03 PFU/cell or uninfected (Co) at indicated time points postinfection. (B) Growth kinetics of the same strains in Vero cells. Cells were infected at an MOI of 0.03 PFU/cell. At the indicated time points, titers were determined for both cell-associated and released viral particles. (C) Western analysis of total cell lysates derived from the cells shown in panel B using anti-H antibodies. (D) Coimmunoprecipitation of F with H from Vero cells infected with the indicated viruses at an MOI of 1.0 PFU/cell. F antigenic material from coimmunoprecipitated samples (IP)and total cell lysate (TL) is shown. (E) The same experiments were carried out as those shown in panel D.7 Cells were infected with MV-H_{Flag} or MV-Edm-H/F-Moraten, followed by treatment with FIP as indicated. Coimmunoprecipated samples (IP) and total cell lysate (TL) are shown.

ters of the different viruses were comparable over time (Fig. 7B), although MV-Moraten and MV-Edm-H/F-Moraten maintained an extended plateau phase of virus production, presumably reflecting less-extensive cell death. Again, expression of MV-H protein over time was consistent with the observed titers, when equal amounts of protein were analyzed by Western blotting (Fig. 7C). Importantly, coimmunoprecipitation experiments revealed that the F and H glycoproteins of the viruses with reduced fusogenicity, MV-Moraten and MV-Edm-H/F-Moraten, form more stable heteromeric complexes than those of MV-Edm (Fig. 7D).

F protein derived from a primary MV isolate strongly interacts with H. In addition to the MV-Moraten-derived glycoproteins, we analyzed the stability of glycoprotein complexes of another recombinant MV-Edm strain, which carries an F protein

isolated from a wild type MV strain, MV-wtF, instead of F-Edm. The recombinant MV-Edm-F-wtF was selected because it was previously shown to replicate nearly as efficiently as the parental MV-Edm virus in CD46-positive cells, but fusogenicity was reduced (14). When lysates of cells infected with this virus were subjected to coimmunoprecipitation, we again observed a far more stable interaction of the two glycoproteins than of MV-Edm, mirroring our findings for MV-Moraten and MV-Edm-H/F-Moraten (Fig. 7D). Thus, a strong interaction between the envelope proteins, as revealed by coprecipitation of H and F, consistently correlates with reduced cell-to-cell fusion.

Strength of MV glycoprotein interaction determines, rather than is determined by, cell-to-cell fusion. Although our data suggest that reduced stability of MV glycoprotein complexes causes increased cell-to-cell fusion, we cannot exclude that the
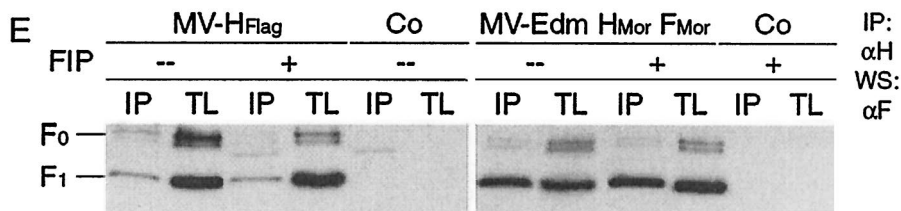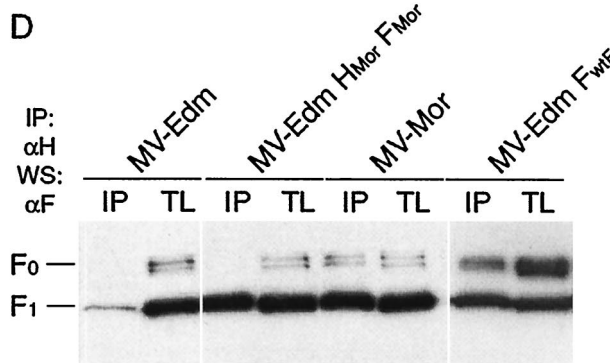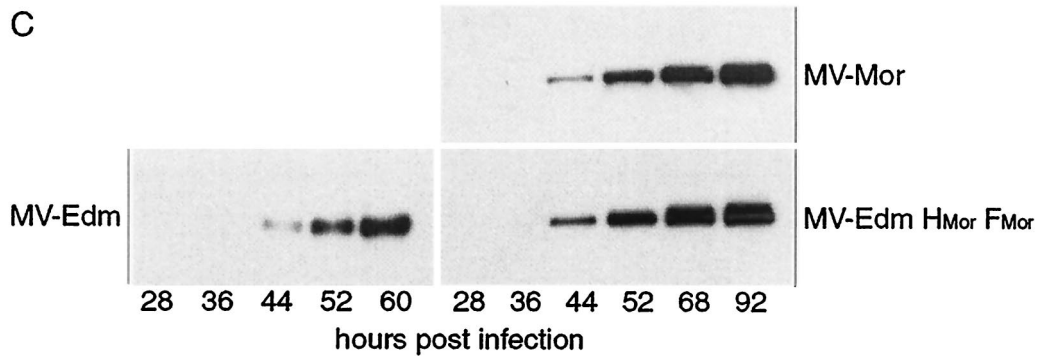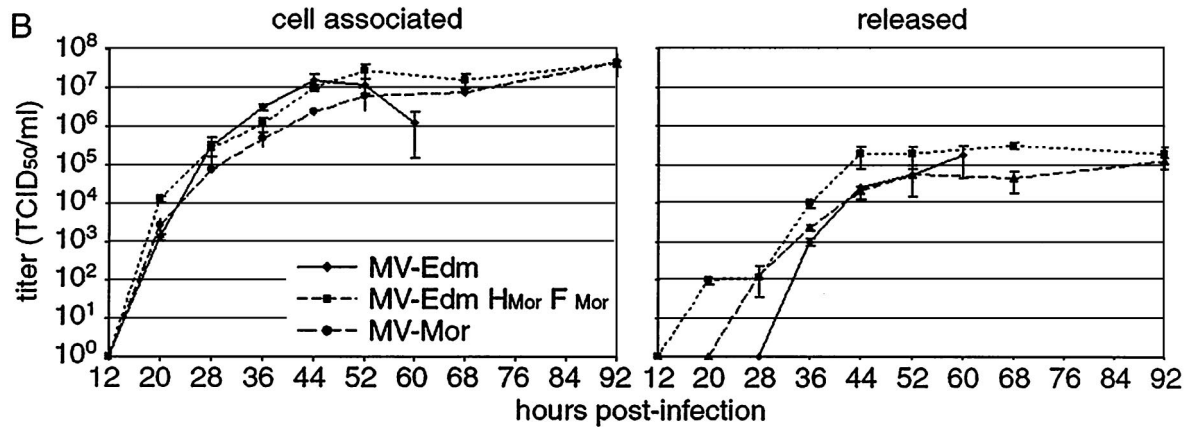
FIG. 7—*Continued.*

fusion event itself provides the mechanistic basis for a reduction of H/F interactions. In this scenario, extensive cell-to-cell fusion, rather than resulting from a weakened interaction, could cause changes in the cellular environment which induce

a destabilization of the complexes. To distinguish between these possibilities, we analyzed the strength of H/F interaction in cells infected with the two viruses displaying the most distinct phenotypes, i.e., MV-H_{Flag} and MV-Edm-H/F-Moraten,

in the presence and absence of FIP, a potent inhibitor of MV-induced cell-to-cell fusion (9).

In infected Vero cells, FIP completely prevented development of syncytia induced by both viruses (data not shown); whereas in the absence of the inhibitor, MV-H_{Flag} induced extensive cell-to-cell fusion and MV-Edm-H/F-Moraten induced its characteristic cell-rounding cytopathic effect described earlier (see Fig. 7A). When assessing the strength of interaction of MV glycoproteins, the H/F coimmunoprecipitation efficiency observed for either virus was virtually identical in both the presence and absence of the inhibitor (Fig. 7E). Consistent with our earlier observations, MV-H_{Flag}-derived H and F displayed a far weaker interaction than the MV-Edm-H/F-Moraten-derived glycoproteins. These data demonstrate that the strength of the MV envelope protein interactions indeed modulates the extent of cell-to-cell fusion, rather than vice versa.

DISCUSSION

We demonstrate that in the context of virus infection the elongation of the MV-H tail by short epitope tags results in a significant increase in lateral cell-to-cell fusion. Our data strongly suggest that the molecular basis for this phenotype lies in a weaker interaction of modified H protein with the F protein, since the coimmunoprecipitation efficiency of the two glycoproteins is significantly reduced in infected cells. Thus, the strength of MV envelope glycoprotein interactions is a modulator of viral cytopathicity.

Several lines of evidence support the modification of the H tail as the basis for the observed phenotype. Firstly, addition of a different epitope tag, HA, in place of Flag results in similar changes in viral phenotype, also demonstrating that the alteration does not depend on the specific sequence appended. Secondly, biochemical data demonstrate a weakened interaction between H-Edm_{Flag} or H-Edm_{HA} and F in both MV-H_{Flag} and MV-H_{HA}. Lastly, no further sequence changes were detected in the H open reading frame of the mutated viruses when analyzed by reverse transcription-PCR and DNA sequencing.

The phenotype of MV-H_{Flag} is distinct from that of previously described MV mutants, since fusogenicity is improved without impairing the efficiency of replication. An MV-Edm derivative lacking M protein also displays an increase in cell-to-cell fusion but has a concomitantly reduced viral titer, particularly of released virus (4). Similarly, MV-Edm, lacking the cytoplasmic tails of both H and F, induces more-extensive lateral fusion but again with some loss in overall titer (5). It was also shown in these studies that the glycoproteins with truncated cytosolic tails were incorporated less efficiently into viral particles. We provide direct biochemical evidence that extending the cytoplasmic tail of MV H in the context of a viral infection impairs its interaction with F but results in both increased fusogenicity and infectivity.

When analyzing glycoproteins derived from different MV strains, attenuated or a primary isolate, we also observed an inverse correlation between lateral spread and cytopathicity and the stringency of glycoprotein interaction. For these experiments, recombinant particles were used that differ exclusively in their glycoproteins but have identical genomic backbones. Usage of receptor molecules other than CD46 by these recombinants as an alternative explanation for our observations appears unlikely because MV-Moraten and MV-Edm-H/F-Moraten grow to titers similar to those of MV-Edm on Vero cells, H-Moraten mutations compared to those of H-Edm do not affect known CD46 binding residues (1, 18), and MV-Edm-F-wtF differs from MV-Edm only in the F protein, which is not involved in viral attachment to target cells. Furthermore, all target cell lines analyzed in our study are CD150 (SLAM) negative.

The MV-M protein interacts with both the F cytosolic tail (33) and ribonucleocapsid (13, 34), presumably linking the viral genome to the glycoproteins. Interestingly, the difference in strength of interaction between H/F and H_{Flag}/F complexes is unchanged in the presence or absence of M. Given that MV glycoprotein hetero-oligomerization already initiates in the endoplasmic reticulum (25), this might occur prior to their interaction with M. Our experiments suggest that presence of ribonucleocapsid results in a destabilization of the H_{Flag}/F glycoprotein complexes, presumably reflecting conformational rearrangements. It is intriguing to speculate that the H cytoplasmic tails could interact directly with ribonucleocapsids. In the presence of H_{Flag} the viral particles were enriched in both M and F proteins while the amount of H was slightly reduced. This increased incorporation of M and F might reflect a tighter binding of M to F cytosolic tails in MV-H_{Flag} particles.

Despite their slightly tighter envelope glycoprotein interaction, viruses lacking the M protein were found to be highly fusogenic (4). This indicates that the modulatory effect of H/F interaction strength on fusogenicity may be mechanistically mediated through a complex interplay between the envelope glycoproteins, M and ribonucleocapsid, and that the strength of glycoprotein interaction constitutes an important parameter for, but is not the only determinant of, fusogenicity.

The increased sensitivity of MV-H_{Flag} particles to neutralization through soluble receptor molecules furthermore suggests an altered conformational state of the H_{Flag}/F complexes. Presumably, the cytosolic epitope tags induce a weakening of the glycoprotein complex stability, which results in a conformational rearrangement of the protein ectodomains increasing the binding affinity to the CD46 receptor and or resembling an activated state that facilitates fusion.

Interestingly, none of the sequence differences between glycoproteins derived from MV-Edm, MV-Moraten, and MV-wtF are localized in the cytosolic domains of the proteins, in contrast to the epitope tags added to the cytosolic tail of H-Edm. Thus, mutations in distant domains of the molecules, cytosolic or extracellular, can influence the stability of the MV-glycoprotein complex and therefore change viral cytopathicity. In conclusion, the strength of MV envelope protein interaction can be considered as a potent modulator of lateral viral spread.

REFERENCES

1. **Bartz, R., U. Brinckmann, L. M. Dunster, B. Rima, V. Ter Meulen, and J. Schneider-Schaulies.** 1996. Mapping amino acids of the measles virus hemagglutinin responsible for receptor (CD46) downregulation. Virology **224:** 334–337.
2. **Calain, P., and L. Roux.** 1993. The rule of six, a basic feature for efficient replication of Sendai virus defective interfering RNA. J. Virol. **67:**4822–4830.
3. **Cathomen, T., C. J. Buchholz, P. Spielhofer, and R. Cattaneo.** 1995. Preferential initiation at the second AUG of the measles virus F mRNA: a role for the long untranslated region. Virology **214:**628–632.
4. **Cathomen, T., B. Mrkic, D. Spehner, R. Drillien, R. Naef, J. Pavlovic, A. Aguzzi, M. A. Billeter, and R. Cattaneo.** 1998. A matrix-less measles virus is infectious and elicits extensive cell fusion: consequences for propagation in the brain. EMBO J. **17:**3899–3908.
5. **Cathomen, T., H. Y. Naim, and R. Cattaneo.** 1998. Measles viruses with altered envelope protein cytoplasmic tails gain cell fusion competence. J. Virol. **72:**1224–1234.
6. **Christiansen, D., P. Devaux, B. Reveil, A. Evlashev, B. Horvat, J. Lamy, C. Rabourdin-Combe, J. H. Cohen, and D. Gerlier.** 2000. Octamerization enables soluble CD46 receptor to neutralize measles virus in vitro and in vivo. J. Virol. **74:**4672–4678.
7. **Dorig, R. E., A. Marcil, A. Chopra, and C. D. Richardson.** 1993. The human CD46 molecule is a receptor for measles virus (Edmonston strain). Cell **75:**295–305.
8. **Enders, J. F., S. L. Katz, M. L. Milovanovic, and A. Holloway.** 1960. Studies of an attenuated measles virus vaccine. N. Engl. J. Med. **263:**153–159.
9. **Firsching, R., C. J. Buchholz, U. Schneider, R. Cattaneo, V. ter Meulen, and J. Schneider-Schaulies.** 1999. Measles virus spread by cell-cell contacts: uncoupling of contact-mediated receptor (CD46) downregulation from virus uptake. J. Virol. **73:**5265–5273.
10. **Granowitz, C., J. Colicelli, and S. P. Goff.** 1991. Analysis of mutations in the envelope gene of Moloney murine leukemia virus: separation of infectivity from superinfection resistance. Virology **183:**545–554.
11. **Hammond, A. L., R. K. Plemper, J. Zhang, U. Schneider, S. J. Russell, and R. Cattaneo.** 2001. Single-chain antibody displayed on a recombinant measles virus confers entry through the tumor-associated carcinoembryonic antigen. J. Virol. **75:**2087–2096.
12. **Hilleman, M. R., E. B. Buynak, R. E. Weibel, J. Stokes, Jr., J. E. Whitman, Jr., and M. B. Leagus.** 1968. Development and evaluation of the Moraten measles virus vaccine. JAMA **206:**587–590.
13. **Hirano, A., M. Ayata, A. H. Wang, and T. C. Wong.** 1993. Functional analysis of matrix proteins expressed from cloned genes of measles virus variants that cause subacute sclerosing panencephalitis reveals a common defect in nucleocapsid binding. J. Virol. **67:**1848–1853.
14. **Johnston, I. C., V. ter Meulen, J. Schneider-Schaulies, and S. Schneider-Schaulies.** 1999. A recombinant measles vaccine virus expressing wild-type glycoproteins: consequences for viral spread and cell tropism. J. Virol. **73:** 6903–6915.
15. **Karlsson, G. B., M. Halloran, J. Li, I. W. Park, R. Gomila, K. A. Reimann, M. K. Axthelm, S. A. Iliff, N. L. Letvin, and J. Sodroski.** 1997. Characterization of molecularly cloned simian-human immunodeficiency viruses causing rapid CD4⁺ lymphocyte depletion in rhesus monkeys. J. Virol. **71:**4218–4225.
16. **Klasse, P. J., R. Bron, and M. Marsh.** 1998. Mechanisms of enveloped virus entry into animal cells. Adv. Drug Deliv. Rev. **34:**65–91.
17. **Kristensson, K., and E. Norrby.** 1986. Persistence of RNA viruses in the central nervous system. Annu. Rev. Microbiol. **40:**159–184.
18. **Lecouturier, V., J. Fayolle, M. Caballero, J. Carabana, M. L. Celma, R. Fernandez-Munoz, T. F. Wild, and R. Buckland.** 1996. Identification of two amino acids in the hemagglutinin glycoprotein of measles virus (MV) that govern hemadsorption, HeLa cell fusion, and CD46 downregulation: phe-

19. notypic markers that differentiate vaccine and wild-type MV strains. J. Virol. **70:**4200–4204.
19. **Mrkic, B., B. Odermatt, M. A. Klein, M. A. Billeter, J. Pavlovic, and R. Cattaneo.** 2000. Lymphatic dissemination and comparative pathology of recombinant measles viruses in genetically modified mice. J. Virol. **74:**1364–1372.
20. **Mulligan, M. J., G. V. Yamshchikov, G. D. Ritter, Jr., F. Gao, M. J. Jin, C. D. Nail, C. P. Spies, B. H. Hahn, and R. W. Compans.** 1992. Cytoplasmic domain truncation enhances fusion activity by the exterior glycoprotein complex of human immunodeficiency virus type 2 in selected cell types. J. Virol. **66:**3971–3975.
21. **Naniche, D., G. Varior-Krishnan, F. Cervoni, T. F. Wild, B. Rossi, C. Rabourdin-Combe, and D. Gerlier.** 1993. Human membrane cofactor protein (CD46) acts as a cellular receptor for measles virus. J. Virol. **67:**6025–6032.
22. **Parks, C. L., R. A. Lerch, P. Walpita, H. P. Wang, M. S. Sidhu, and S. A. Udem.** 2001. Comparison of predicted amino acid sequences of measles virus strains in the Edmonston vaccine lineage. J. Virol. **75:**910–920.
23. **Piller, S. C., J. W. Dubay, C. A. Derdeyn, and E. Hunter.** 2000. Mutational analysis of conserved domains within the cytoplasmic tail of gp41 from human immunodeficiency virus type 1: effects on glycoprotein incorporation and infectivity. J. Virol. **74:**11717–11723.
24. **Plemper, R. K., A. L. Hammond, and R. Cattaneo.** 2000. Characterization of a region of the measles virus hemagglutinin sufficient for its dimerization. J. Virol. **74:**6485–6493.
25. **Plemper, R. K., A. L. Hammond, and R. Cattaneo.** 2001. Measles virus envelope glycoproteins hetero-oligomerize in the endoplasmic reticulum. J. Biol. Chem. **4:**4.
26. **Radecke, F., P. Spielhofer, H. Schneider, K. Kaelin, M. Huber, C. Dotsch, G. Christiansen, and M. A. Billeter.** 1995. Rescue of measles viruses from cloned DNA. EMBO J. **14:**5773–5784.
27. **Rahman, S. M., H. Eto, S. A. Morshed, and H. Itakura.** 1996. Giant cell pneumonia: light microscopy, immunohistochemical, and ultrastructural study of an autopsy case. Ultrastruct. Pathol. **20:**585–591.
28. **Rota, J. S., Z. D. Wang, P. A. Rota, and W. J. Bellini.** 1994. Comparison of sequences of the H, F, and N coding genes of measles virus vaccine strains. Virus Res. **31:**317–330.
29. **Sakaguchi, M., Y. Yoshikawa, K. Yamanouchi, T. Sata, K. Nagashima, and K. Takeda.** 1986. Growth of measles virus in epithelial and lymphoid tissues of cynomolgus monkeys. Microbiol. Immunol. **30:**1067–1073.
30. **Shinohara, K., K. Sakai, S. Ando, Y. Ami, N. Yoshino, E. Takahashi, K. Someya, Y. Suzaki, T. Nakasone, Y. Sasaki, M. Kaizu, Y. Lu, and M. Honda.** 1999. A highly pathogenic simian/human immunodeficiency virus with genetic changes in cynomolgus monkey. J. Gen. Virol. **80:**1231–1240.
31. **Singh, M., and M. A. Billeter.** 1999. A recombinant measles virus expressing biologically active human interleukin-12. J. Gen. Virol. **80:**101–106.
32. **Spehner, D., R. Drillien, and P. M. Howley.** 1997. The assembly of the measles virus nucleoprotein into nucleocapsid-like particles is modulated by the phosphoprotein. Virology **232:**260–268.
33. **Spielhofer, P., T. Bachi, T. Fehr, G. Christiansen, R. Cattaneo, K. Kaelin, M. A. Billeter, and H. Y. Naim.** 1998. Chimeric measles viruses with a foreign envelope. J. Virol. **72:**2150–2159.
34. **Suryanarayana, K., K. Baczko, V. ter Meulen, and R. R. Wagner.** 1994. Transcription inhibition and other properties of matrix proteins expressed by M genes cloned from measles viruses and diseased human brain tissue. J. Virol. **68:**1532–1543.
35. **Thormar, H., P. D. Mehta, and H. R. Brown.** 1978. Comparison of wild-type and subacute sclerosing panencephalitis strains of measles virus. Neurovirulence in ferrets and biological properties in cell cultures. J. Exp. Med. **148:**674–691.
36. **Yang, C., and R. W. Compans.** 1996. Analysis of the cell fusion activities of chimeric simian immunodeficiency virus-murine leukemia virus envelope proteins: inhibitory effects of the R peptide. J. Virol. **70:**248–254.
37. **Zingler, K., and D. R. Littman.** 1993. Truncation of the cytoplasmic domain of the simian immunodeficiency virus envelope glycoprotein increases *env* incorporation into particles and fusogenicity and infectivity. J. Virol. **67:** 2824–2831.